Progress In Electromagnetics Research, Vol. 129, 541–558, 2012

AN EXPERIMENTAL MULTI-FREQUENCY SYSTEM FOR STUDYING DOSIMETRY AND ACUTE EFFECTS ON CELL AND NUCLEAR MORPHOLOGY IN RAT TISSUES

A. López Furelos[1], M. M. Miñana Maiques[2], J. M. Leiro[3], J. A. Rodríguez-González[4], F. J. Ares-Pena[4], and E. López-Martín[1, *]

[1]Department of Morphological Sciences, University of Santiago de Compostela, Santiago de Compostela 15782, Spain

[2]SPEAG Schmid & Partner Engineering AG, Zurich, Switzerland

[3]Institute of Food Research and Analysis, University of Santiago de Compostela, Santiago de Compostela 15782, Spain

[4]Department of Applied Physics, University of Santiago de Compostela, Santiago de Compostela 15782, Spain

Abstract—Simultaneous exposure to multiple electromagnetic signals with widely differing carrier frequencies is a reality of daily life, but its possible effects on health are unknown. In this study, we exposed rats to non-thermal levels of 900 and 2450 MHz TEM-mode radiation, applied individually or simultaneously, and we obtained estimates of 1 g mean SAR (specific absorption rate) in various tissues using a numerical model of the rat and finite-difference time-domain software. The experimental system comprised a GTEM (gigahertz TEM) chamber connected to two vector signal generators, a signal mixer and amplifier, a directional coupler, a spectrum analyzer and a power meter. Tissue sections from rats sacrificed 24 h after exposure, and from negative controls and positive controls exposed to gamma radiation, were stained with haematoxylin-eosin for evaluation of general cell morphology and with DAPI (4', 6-diamidino-2-phenylindole) for evaluation of apoptosis. Lesions, tissue destruction and apoptosis were only observed in positive controls. The results for rats exposed to either frequency, or to both simultaneously, were similar to those of unexposed negative controls. It remains to determine whether chronic exposure is similarly innocuous.

Received 27 April 2012, Accepted 4 July 2012, Scheduled 12 July 2012

* Corresponding author: Elena López-Martin (melena.lopez.martin@usc.es).

1. INTRODUCTION

Electromagnetic (EM) fields are a vital part of our daily lives. The presence of various kinds of antenna in towns and cities, including cell phone antennas, exposes the majority of the population to radiation of multiple frequencies, especially radio frequencies (RF). In spite of this, there has been very little research on the biological effects of simultaneous EM signals. In particular, legal limits on the specific absorption rate (SAR) associated with exposure to multiple signals [1] have not been based on experimental evidence, and there is accordingly significant uncertainty regarding the effectiveness of these limits.

The few studies there have been in this area have not clearly identified potential health risks related to multiple RF exposure: no relationship has been established between multifrequency exposure and cellular alterations in embryos during gestation [2], alteration of testicular function [3], toxic or carcinogenic effects [4, 5], or chronic symptoms such as headaches or sleep alterations in adults [6] and children [7]. Nevertheless, the paucity of information on the possible bio-effects of multiple RF signals contrasts with the concern of the general public and of various governmental entities [8, 9].

In this study, we aimed 1) to develop an experimental system for simultaneous exposure of small animals to multiple RF signals; 2) to obtain SAR estimates for various tissues of rats exposed in the system to simultaneous signals at the frequencies habitually used by wireless communication systems, 900 and 2450 MHz; 3) to observe the state and apoptosis status of those tissues in the experimentally exposed rats; and 4) to examine possible correlation between tissue damage and SAR-based absorption estimates. SAR estimates were obtained by finite-difference time-domain (FDTD) calculations using SEMCAD commercial software [10] with a numerical phantom (model) of the rat.

2. MATERIAL AND METHODS

2.1. Animals

The animals used in this study were adult male Sprague-Dawley rats weighing 230–250 g. They were housed in individual cages, with free access to food and water, in an environment maintained at 22°C and subjected to a 12 : 12 h light/dark regime. All experiments were carried out in accordance with European regulations on animal protection (Directive 86/609), the Declaration of Helsinki and/or the Guide for the Care and Use of Laboratory Animals, as adopted and promulgated by the US National Institutes of Health (NIH Publication No. 85–23, revised 1996). All experimental protocols were approved by the

Institutional Animal Care and Use Committee of the University of Santiago de Compostela.

2.2. Experimental Setup, and Calculation of SARs

2.2.1. The Experimental Radiation System

Figure 1 shows the experimental setup. Two vector signal generators, VSG1 and VSG2, generate pure sinusoidal signals of 2450 and 900 MHz, respectively, at the required power levels. Their outputs are combined in a signal mixer (SM), and the signal is then passed through an amplifier (AMP) and a directional coupler (DC) before entering the $125 \times 65 \times 35$ cm GTEM radiation chamber [11], where the rat (R), immobilized in a plexiglass holder (RH), is positioned in the region of maximum field uniformity (approximately $15 \times 15 \times 8$ cm for a maximum variation of 3 dB) [12]. Despite this position, since the EM wave hits the rat broadside (with **E** perpendicular and **H** parallel to its midline), its right side is to some degree shielded by its left side.

The DC enables measurement of incident power values (P_{IN}) by the power meter (PM) and of reflected power (P_{REF}) by the spectrum analyser (SA); the SA also enables observation of the wave configuration in the chamber and hence verification of spectral purity. An isotropic probe (IP) is used to map the field in the ratless chamber, which serves not only to identify the optimal position of the rat, but also to calibrate input power and the parameters of the simulations used for SAR estimation. It is preferable to use these measurements rather than the field formula recommended by the chamber manufacturer [12] because the latter, $E = \sqrt{Z_0 P_{\mathrm{TR}}/(h^2\zeta)}$ (where h is the height of the septum at the position of the rat, $P_{\mathrm{TR}} = P_{\mathrm{IN}} - P_{\mathrm{REF}}$, $Z_0 = 50$ [Ω] is the GTEM input impedance, and ζ is a ripple-dependent coefficient that is taken equal to 2 [12]), fails to take into account the presence of more than one frequency.

2.2.2. Simulations

The SAR values were estimated by the FDTD method [13, 14] using the simulation software package SEMCAD X [6] and a numerical model of a 198.3 gram Sprague-Dawley rat (model R8 [10]) that had been assembled from 1.15 mm magnetic resonance sections and distinguished among 60 different tissues. Simulated plane waves were generated to reproduce the measured field. Simulations at 900 MHz used 2.5 million volumetric cells and took 20 minutes on a desktop PC with a 3.2 GHz i7 Intel Core processor, 16 GB of RAM and an Nvidia Tesla C1060 accelerator card, while simulations at 2450 MHz

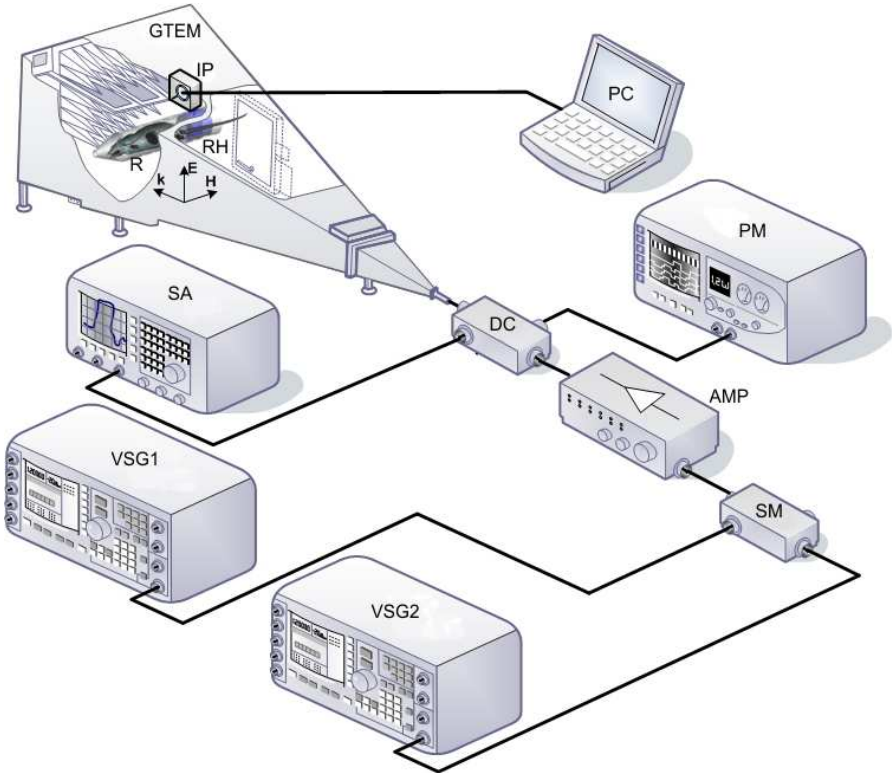

Figure 1. Schematic of the system. GTEM, Schaffner 250 GTEM chamber; VSG1, Agilent E8267D vector signal generator (250 KHz–20 GHz) operating at 2.45 GHz; VSG2, Agilent E4438C vector signal generator (250 KHz–4 GHz) operating at 900 MHz; AMP, research amplifier 15S1G3 (0.8–3 GHz); DC, NARDA 3282B-30 directional coupler (800–4000 MHz); SA, Agilent E4407B spectrum analyzer (9 KHz–26.5 GHz); PM, Agilent E4418B power meter; SM, Agilent 11636[a] signal mixer; RH, rat holder; IP, EF Cube isotropic probe; R, rat.

used 20.3 million volumetric cells and took 35 minutes. SAR values were obtained as peak 1 g averages in the tissue of interest, as per IEEE-1529. SARs for simultaneous irradiation with 900 and 2450 MHz signals were calculated as the average of the separate 900 and 2450 MHz SARs.

To obtain SAR estimates for the experimental rats, the values obtained for the numerical phantom were adjusted assuming uniform

inverse dependence on total body weight:

$$\mathrm{SAR}_E = \mathrm{SAR}_S \times W_S/W_E \tag{1}$$

where SAR_E is the estimate for an experimental rat of weight W_E [g], SAR_S is the SAR obtained for the phantom in the simulation, and $W_S = 198.3$ [g] is the weight of the phantom.

2.3. Experimental Design

A total of 30 rats divided in three groups of 10 were individually exposed to radiation in the GTEM chamber.

— **Group 1**: Irradiation at 900 MHz ($P_{\mathrm{TR}} = 2$ W).

— **Group 2**: Irradiation at 2450 MHz ($P_{\mathrm{TR}} = 2$ W).

— **Group 3:** Simultaneous irradiation at 900 MHz ($P_{\mathrm{TR}} = 1$ W) and 2450 MHz ($P_{\mathrm{TR}} = 1$ W).

In addition, two control groups were included in the study:

— **Group 4** comprised 10 rats that were not irradiated (negative controls);

— **Group 5** comprised 6 rats that were exposed to a full-body, 2 Gy dose of gamma radiation for 5 minutes and were slaughtered 6 hours later (positive controls).

All animals of groups 1–4 were immobilised in the rat holder for 1 h (see Fig. 1), during which time the rats in groups 1–3 were individually irradiated. Immobilized group 4 animals were placed in the GTEM chamber but were not irradiated. Rats of groups 1–4 were slaughtered 24 h after removal from the GTEM chamber.

Haematoxylin-eosin-stained rat tissue sections prepared as described below were examined under a conventional microscope at 40X and 100X magnifications for evaluation of the general organization and cell morphology of the tissue in question. Sections stained with DAPI (4', 6-diamidino-2-phenylindole dihydrochloride) were examined under a fluorescence microscope for evaluation of nuclear morphology. In both cases the sections were evaluated by a researcher who was blind to their group of origin.

2.4. Tissue Extraction and Preparation

After radiation, the rats rested for 24 hours and were then slaughtered by intra-peritoneal injection of sodium pentothal (to diminish stress levels) followed by an overdose of ethyl ether and immediate perfusion via the ascending aorta with paraformaldehyde at 4°C. The cerebral cortex, cerebellum, pituitary gland, tongue, trapezoid muscle, thymus,

interscapular fat and a testicle were then extracted and immersed in fixative solution (10% formaldehyde in phosphate buffer). Tissues were prepared for microscopy using standard techniques, as follows.

After 4 hours in fixative solution, tissues were dehydrated for embedding in paraffin by transfer to para-formaldehyde, refrigeration at 4°C for 24 hours, transfer to 70° alcohol for 2 hours and then to fresh 70° alcohol, stirring for 12 hours, and then successive transfer to 90° alcohol for 2 hours, to fresh 90° alcohol for 2 hours, to 100° alcohol for 2 hours, and to fresh 100° alcohol for 1 hour. After clearing in toluene for 12 hours, the tissues were then embedded by three successive immersions in paraffin wax.

The embedded tissues were cut in 5 μm sections with a microtome, and the sections were mounted on microscope slides and dried in an oven at 37° for at least 24 hours.

General tissue organization and cell morphology were examined in sections stained with haematoxylin-eosin as follows. The sections were deparrafinated by heating in an oven at 60° for 30 minutes, and then transferred successively to xylol (2×5 min), 100° alcohol (2×5 min), 96° alcohol (2 × 5 min), 70° alcohol (1 × 5 min), and distilled water. They were then transferred to haematoxylin solution for 10 min, washed under running tap water for 10 min, and finally transferred to eosin solution for 5 min before redehydration by passage through 90° alcohol (2 × 1 min), 100° alcohol (2 × 1 min) and xylol (2 × 5 min). They were then mounted, covered and code-labelled pending microscopic examination.

For examination of nuclear morphology, sections were deparaffinated and rehydrated as described in the previous paragraph, transferred for 15 min to a 0.8 mg/ml solution of 4', 6-diamidino-2-phenylindole dihydrochloride (DAPI; Sigma-Aldrich) in phosphate-buffered saline (PBS), and then washed several times in PBS before being mounted, covered and code-labelled for microscopic examination.

3. RESULTS

3.1. SAR Estimates

The optimal position of rats in the GTEM chamber was found to be where the height of the septum above the chamber floor was 0.215 m. Figs. 2, 3 and 4 show maps of 1 g average SAR in the numerical rat phantom for radiation at respectively 900 MHz, 2450 MHz, and both frequencies simultaneously. Asymmetry due to the shielding of the rat's right side by its left side adds to that resulting from asymmetric distribution of organs.

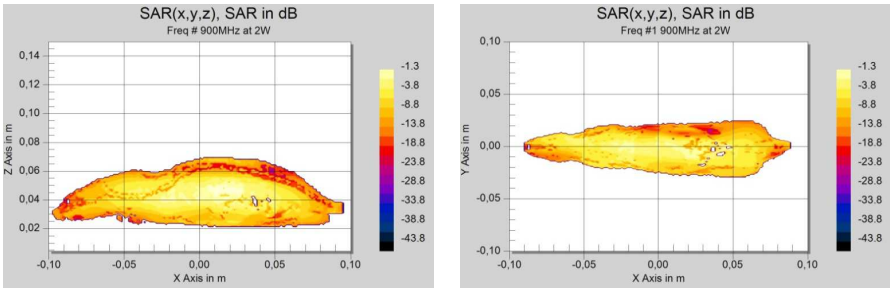

Figure 2. Distribution of 1 g average SAR in vertical and horizontal sections of the numerical rat phantom when radiated at 900 MHz ($P_{\mathrm{TR}} = 2\,\mathrm{W}$). SAR is expressed relative to absorption of the entire local power density in the absence of the rat.

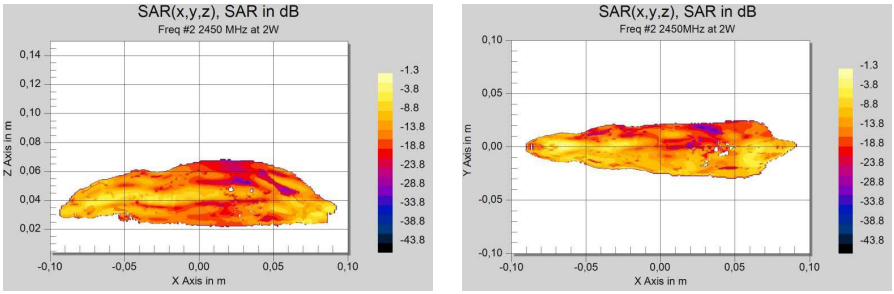

Figure 3. Distribution of 1 g average SAR in vertical and horizontal sections of the numerical rat phantom when radiated at 2450 MHz ($P_{\mathrm{TR}} = 2\,\mathrm{W}$). SAR is expressed relative to absorption of the entire local power density in the absence of the rat.

Table 1 lists the experimental conditions, weights and estimated whole-body peak SAR values obtained for the various experimental groups, and Table 2 the estimated peak SAR values for individual tissues.

3.2. Histopathological Results

3.2.1. Haematoxylin-eosin-stained Sections

Figure 5 shows details of typical haematoxylin-eosin-stained sections of the eight types of tissue examined. In all cases, the evident damage caused by gamma radiation in group 5 contrasts with the absence or near-absence of any pathological signs in tissues from the other groups.

— In groups 1–4 the cerebral cortex, cerebellum and pituitary

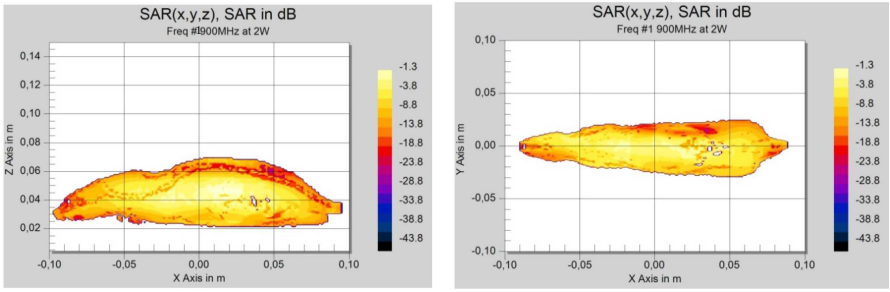

Figure 4. Distribution of 1 g average SAR in vertical and horizontal sections of the numerical rat phantom when radiated simultaneously with 900 MHz ($P_{\mathrm{TR}} = 1$ W) and 2450 MHz ($P_{\mathrm{TR}} = 2$ W). SAR is expressed relative to absorption of the entire local power density in the absence of the rat.

gland showed at most faint traces of haemorrhage (isolated red blood cells), with no increase in dark neurons or visible signs of apoptosis. By contrast, sections from group 5 showed significant haemorrhage, an increase in dark neurons and, in neurons of the cerebral cortex, intracytoplasmic aggregates. Signs of apoptosis and neuron destruction in these tissues in group 5 included the decreased size of the nuclei of pituitary neurons and smaller numbers of Purkinje cells in the cerebellum.

— The tongues of group 5 animals showed signs of lesions that included haemorrhage and microphages in the submucosal layer, a decrease in the thickness of the epithelium, and an increase in the number of apoptotic nuclei. Animals of groups 1–4 showed no visible signs of cell lesion, haemorrhage or apoptosis in either mucous or muscle layers.

— The interscapular fat of groups 1–4 exhibited the typical hexagonal morphology of adipocytes in different phases of development, along with undifferentiated fatty tissue cells. In group 5, adipocytes had lost their hexagonal morphology and shrunk, there were fewer early-phase adipocytes, and haemorrhage was abundant.

— In the trapezoid muscle tissue of groups 1–3 the nuclei retained their morphology, presented no signs of cellular destruction or haemorrhage, and were in all other respects likewise histologically similar to that of group 4, in sharp contrast to the cell destruction, abundant haemorrhage, morphological changes and nuclear disaggregation of group 5 muscle tissue.

Table 1. Experimental conditions, [a] weights, and estimated whole-body peak 1 g average SARs of the experimental groups subjected to RF radiation.

	f [MHz]	P_{TR} [W]	E_m [V/m]	W_E [g]	SAR_E [W/kg] (Whole-body)
GROUP 1	900	2	47.5	**Min.** 182.9	0.1587
				Max. 218.8	0.1898
				Mean 198.7	0.1718
GROUP 2	2450	2	40.2	**Min.** 198.1	0.0601
				Max. 243.7	0.0740
				Mean 224.7	0.0683
GROUP 3	900 + 2450	1 + 1	34.4	**Min.** 153.4	0.0879
				Max. 306.3	0.1755
				Mean 230.8	0.1322

[a] f, frequency; P_{TR}, transmitted power (see Subsubection 2.2.1); E_m, measured r.m.s. electrical field strength.

— In groups 1–4 the external morphology of the thymic cortex and medulla was normal, as were the lymphocyte populations and Hassall's corpuscles. Reticulo-endothelial cells were few (most abundant in group 3), and isolated non-active macrophages appeared sporadically. The thymi of group 5 rats showed clear signs of haemorrhage in the cortex and medulla, along with changes in medullary structure consisting in an increase in connective tissue and decreased cellularity. Group 5 also exhibited increased auto-immune activity, with abundant, active macrophages and an increase in reticulo-epithelial cells in all layers.

— Dynamic spermatogenesis in the testicles of group 1–4 animals was shown by the observation of spermatocytes of different

Table 2. Group mean estimated tissue-specific peak 1 g average SARs.

TISSUE	GROUP 1	GROUP 2	GROUP 3
Cerebral hemispheres	0.0902	0.0749	0.1009
Pituitary	0.2088	0.2633	0.3139
Cerebellum	0.2152	0.0981	0.1551
Trapezoid muscle	0.1601	0.0654	0.1130
Thymus	0.2880	0.0637	0.1755
Testicle	0.0902	0.2870	0.2165
Interscapular fat	0.0323	0.0195	0.0266
Tongue	0.1215	0.2402	0.1740

developmental stages. Group 5 testicle exhibited more primary spermatocytes but hardly any advanced spermatids in the semeniferous conducts, along with decreased spermatogenesis and an increase in cellular apoptosis and the number of fragmented nuclei.

3.2.2. DAPI-stained Nuclei

Examination of DAPI-stained tissues at 100X under a fluorescence microscope showed the following features of nuclear morphology (Fig. 6).

— In cerebral cortex, cerebellum and pituitary gland from animals of groups 1–4, signs of apoptosis (chromatin condensation or DNA fragmentation) were rare, appearing in fewer than 3% of cells in group 3 cerebellum. The neuronal nuclei of animals exposed to ionizing gamma radiation (group 5) exhibited clustered material.

— Apoptosis rates in the tongues of animals radiated with just a single frequency (groups 1 and 2) were insignificant and similar to those of non-exposed group 4 animals. Apoptosis was more frequent in group 3 tongue, but never exceeded 4% (found in mucous epithelial cells. Animals exposed to gamma radiation exhibited much higher apoptosis rates.

— In groups 1–4 fewer than 4% of interscapular fatty tissue cells were apoptotic, whereas group 5 levels were much higher.

— The trapezoid muscles, thymi and testicles of groups 1–4 showed few or no signs of apoptosis. By contrast, apoptosis was common in these tissues in the positive control animals of group 5, as shown by deformed or fragmented nuclei.

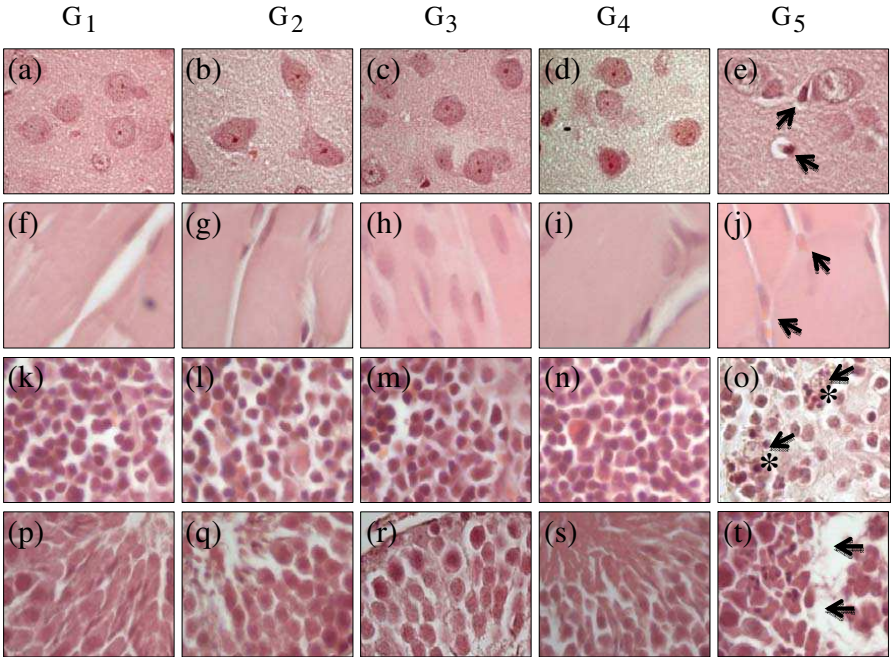

Figure 5. Tissue sections stained with haematoxylin-eosin, showing the cerebral cortex (a)–(e), trapezoid muscle (f)–(j), thymus (k)–(o) and testicular seminiferous ducts (p)–(t) of rats of groups 1–5 (columns G1–G5, respectively). The tissues of animals exposed to 0.9 GHz (G1), 2.4 GHz (G2) and 0.9 and 2.45 GHz simultaneously (G3) were similar to those of the non-irradiated negative control group (G4) in their appearance and the minimal prevalence of signs of lesions. In photomicrographs of sections from rats exposed to gamma radiation (G5), arrows or asterisks indicate the presence of dark neurons in cerebral cortex (e), red blood cells in trapezoid muscle (j), active macrophages interacting with other cells in thymus (o), and signs of destruction in the seminiferous ducts (t). 100X.

4. DISCUSSION

In this research, we 1) developed a multi-frequency radiation test system allowing simultaneous exposure of rats and similarly sized animals to EM signals of two different frequencies in the 800–2700 MHz band; 2) obtained SAR values for representative tissues of a standard rat irradiated at 900 MHz, 2450 MHz and an equipotent combination of these two frequencies ($P_{\mathrm{TR}} = 2\,\mathrm{W}$), and scaled these SAR values

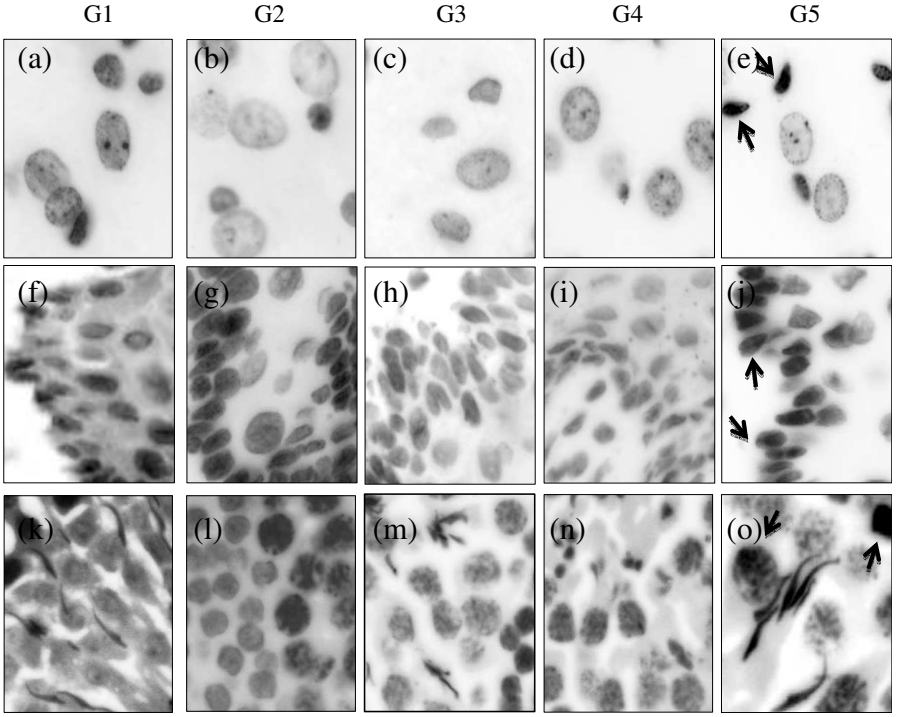

Figure 6. Grey-scale photomicrographs of DAPI-stained sections of the cerebral cortex (a)–(e), lingual mucous membrane (f)–(j) and testicular seminiferous ducts (k)–(o) of rats of groups 1–5 (columns G1–G5, respectively). The tissues of animals exposed to 0.9 GHz (G1), 2.45 GHz (G2) and 0.9 and 2.45 GHz simultaneously (G3) had similar nuclear integrity to those of the non-irradiated negative control group (G4). In photomicrographs of sections from rats exposed to gamma radiation (G5), arrows indicate dark neurons typical of pre-apoptotic states in the cerebral cortex (e), and apoptotic cells in the lingual mucosa (j) and testicular seminiferous ducts (o). 100x.

for experimental rats; and 3) observed the effects of the two-frequency signal on the cells of these tissues in comparison with the effects of the single-frequency signals, gamma radiation, or non-exposure. In conformity with Spanish [1] and international [8] legislation, and with the few previous studies of multifrequency exposure, SAR values for exposure to the mixed signal were calculated as the appropriately power-weighted average of those of the single-frequency exposures. The non-detection of biological effects of EM radiation in the experiments

with rats prevented evaluation of whether this averaging procedure is really valid, of whether the effects of multifrequency signals, when they occur, differ in any way from those of the individual component frequencies, and of whether estimated absorption correlates with biological effects at the exposure levels employed (our fourth initial objective). Since different organs are not all equally sensitive to EM radiation (if only because of their different anatomical locations), we examined the effects of radiation in eight different tissues.

Since the region of the human body that absorbs most energy during the use of a cell phone is the head, there has been extensive research on the effects of non-ionizing radiation of cell phone frequencies on small mammal head and nervous system tissues. Authors working at 900 or 2450 MHz have reported that acute effects in the cerebral cortex and striatum, such as glyosis, neuronal activation and cell stress, are associated with SARs ranging from brain averages of 6.0 W/kg to 1-g-average peaks as low as 0.3 W/kg [15–17]. Alterations in neuronal apoptosis rates or non-caspase-dependent apoptotic pathways have also been observed after single or repeated exposure of whole rats or human or animal neuronal cell lines [18–22]. In other studies, however, no biological effects of 0.8–2.0 GHz radiation on apoptosis have been observed in nervous system tissue [23–25].

The effects of electromagnetic radiation on germ cells and male fertility have been the subject of numerous studies prompted by the common practice of carrying a cell phone in a pocket close to the testicles. In 28-day-old rats, reduced spermatogenesis has been observed after repeated exposure to 0.9 or 2.45 GHz radiation, together with decreased numbers of Leydig cells and increased oxidative stress and apoptosis in testicular tissue [26, 27]. Once more, however, the available information is contradictory, no morphological or biochemical indications of increased apoptosis [5, 28] or of pre-apoptotic states with increased caspase activity [29, 30] having been observed in male sexual cells in other studies after exposure of animals to single or combined radio frequencies.

Lymphoid organs such as the thymus appear to be particularly sensitive to EM fields. Immature rats have been found to have high levels of irreversible oxidative stress after exposure to 900 MHz radiation [31], and repeated exposure at 42 GHz has been associated with altered immunogenic response [32]. Thymic involution during prolonged exposure to 50 Hz radiation [33] is accelerated by continuous light exposure [34].

Fatty tissue is also sensitive to radio frequencies: adipocyte lysis has been observed after repeated exposure to 2.4 MHz microwaves [35], and inflammation and decreased cell counts may be seen at 6 MHz [36].

Repeated exposure of skeletal muscle to 2.45 GHz radiation has been found to cause fatigue and a decrease in acetylcholinesterase activity [37, 38], and to reduce muscle volume [39]. Nevertheless, a relevant review named several *in vitro* and chronic *in vivo* studies of multiple animal tissues that found no increase in cellular apoptosis in response to exposure to non-thermal 800–3000 MHz RF [40].

Real-world exposure to electromagnetic contamination in public or private spaces does not usually involve a single frequency, but the interaction of several radio frequencies [41]. There have been several reports that non-thermal levels of RF radiation can increase apoptosis in response to ionizing ultra-violet or gamma radiation [42, 43]. Studies investigating whether such synergism extends to exposure to multiple radio frequencies have been few, and their results, like ours, negative, whether epidemiological [2, 3] or experimental [4–7]. In the present case, the absence of significant effects may have been due in part to the low specific absorption rates employed (< 0.3 W/kg except in the pituitary glands of group 3) and the use of just a single exposure period rather than repeated exposures. The multifrequency radiation system designed for this study will facilitate the performance of further experiments aimed at a more complete characterization of biological effects in animals exposed to multifrequency RF radiation.

ACKNOWLEDGMENT

The authors thank the Directorate General for Research and Development of the Xunta de Galicia for partial funding of this research through projects 09TIC006206PR and INCITE09E2R206059ES. We greatly appreciate the technical assistance of Rafael Fuentes and Isabel Tarrio.

REFERENCES

1. REAL DECRETO 1066/2001, *Boletín Oficial de Estado*, Sept. 28, 2001.
2. Lee, H. J., J. S. Lee, J. K. Pack, H. D. Choi, N. Kim, S. H. Kim, and Y. S. Lee, "Lack of teratogenicity after combined exposure of pregnant mice to CDMA and WCDMA radio frequency electromagnetic fields," *Radiat. Res.*, Vol. 172, No. 5, 648-52, 2009.
3. Lee, H. J., Y. B. Jin, T. H. Kim, J. K. Pack, N. Kim, H. D. Choi, and Y. S. Lee, "The effects of simultaneous combined exposure to CDMA and WCDMA electromagnetic fields on rat testicular function," *Bioelectromagnetics*, 2011.

4. Lee, H. J., Y. B. Jin, J. S. Lee, S. Y. Choi, T. H. Kim, J. K. Pack, H. D. Choi, N. Kim, and Y. S. Lee, "Lymphoma development of simultaneously combined exposure to two radio frequency signals in AKR/J mice," *Bioelectromagnetics*, Vol. 32, No. 6, 485-92, 2011.
5. Jin, Y. B., H. J. Lee, J. S. Lee, J. K. Pack, N. Kim, and Y. S. Lee, "One year simultaneous combined exposure of CDMA and WCDMA radio frequency electromagnetic fields to rats," *Int. J. Radiat. Biol.*, Vol. 87, No. 4, 416-23, 2011.
6. Thomas, S., A. Kühnlein, S. Heinrich, G. Praml, D. Nowak, R. Von Kries, and K. Radon, "Personal exposure to mobile phone frequencies and well-being in adults: A cross-sectional study based on dosimetry," *Bioelectromagnetics*, Vol. 29, 463–470, 2008.
7. Thomas, S., A. Kühnlein, S. Heinrich, G. Praml, R. Von Kries, and K. Radon, "Exposure to mobile telecommunication networks assessed using personal dosimetry and well-being in children and adolescents: The German mobile study," *Environmental Health*, 2008, http://www.ehjournal.net/content/7/1/54.
8. ICNIRP, International Commission on Non-ionizing Radiation Protection, "Guidelines for limiting exposure to time-varying electric, magnetic, and electromagnetic fields (up to 300 GHz)," *Health Physics*, Vol. 74, 494–522, 1998.
9. Genc, O., M. Bayrak, and E. Yaldiz, "Analysis of the effects of GSM bands to the electromagnetic pollution in the RF spectrum," *Progress In Electromagnetics Research*, Vol. 101, 17–32, 2010.
10. Schmid & Partner Engineering AG, "Reference manual for the SEMCAD simulation platform for electromagnetic compatibility, antenna design and dosimetry," 2010, www.semcad.com.
11. Li, K., Y. Hui, S. Ma, G. Ding, Y. Guo, J. Liu, Y. Li, and G. Guo, "Inhibition of bone formation by high intensity pulsed electromagnetic field in mc3t3-e1 cells," *Progress In Electromagnetics Research*, Vol. 112, 139–153, 2011.
12. Schaffner Electrotest GmbH, "GTEM test cells," GTEM Catalogue, 2005, www.schaffner.com.
13. Zhang, M. and A. Alden, "Calculation of whole-body SAR from a 100 MHz dipole antenna," *Progress In Electromagnetics Research*, Vol. 119, 133–153, 2011.
14. Mohsin, S. A., "Concentration of the specific absorption rate around deep brain stimulation electrodes during MRI," *Progress In Electromagnetics Research*, Vol. 121, 469–484, 2011.
15. Mausset-Bonnefont, A. L., H. Hirbec, X. Bonnefont, A. Privat,

J. Vignon, and R. de Seze, "Acute exposure to GSM 900-MHz electromagnetic fields induces glial reactivity and biochemical modifications in the rat brain," *Neurobiol. Dis.*, Vol. 17, No. 3, 445–454, 2004.

16. López-Martín, E., J. C. Bregains, F. J. Jorge-Barreiro, J. L. Sebastián-Franco, E. Moreno-Piquero, and F. Ares-Pena, "An experimental set-up for measurement of the power absorbed from 900 MHz GSM standing waves by small animals, illustrated by application to picrotoxin treated rats," *Progress In Electromagnetics Research*, Vol. 87, 149–165, 2008.
17. Jorge-Mora, M. T., M. Alvarez-Folgueiras, J. Leiro, F. J. Jorge-Barreiro, F. J. Ares-Pena, and E. Lopez-Martín, "Exposure to 2.45 GHz microwave radiation provokes cerebral changes in induction of HSP90 α/β heat shock protein in rat," *Progress In Electromagnetics Research*, Vol. 100, 351-379, 2010.
18. Kesari, K. K., S. Kumar, and J. Behari, "900-MHz microwave radiation promotes oxidation in rat brain," *Electromagn. Biol. Med.*, Vol. 30, No. 4, 219-34, 2011.
19. Dasdag, S., M. Z. Akdag, E. Ulukaya, A. K. Uzunlar, and A. R. Ocak, "Effect of mobile phone exposure on apoptotic glial cells and status of oxidative stress in rat brain," *Electromagn. Biol. Med.*, Vol. 28, No. 4, 342-54. 2009.
20. Calabrò, E., S. Condello, M. Currò, N. Ferlazzo, D. Caccamo, S. Magazù, and R. Ientile, "Modulation of heat shock protein response in SH-SY5Y by mobile phone microwaves," *R. World J. Biol. Chem.*, Vol. 3, No. 2, 34–40, 2012.
21. Joubert, V., S. Bourthoumieu, P. Leveque, and C. Yardin, "Apoptosis is induced by radio frequency fields through the caspase-independent mitochondrial pathway in cortical neurons," *Radiat. Res.*, Vol. 169, No. 1, 38–45, 2008.
22. Zhao, T. Y., S. P. Zou, and P. E. Knapp, "Exposure to cell phone radiation up-regulates apoptosis genes in primary cultures of neurons and astrocytes," *Neurosci. Lett.*, Vol. 412, No. 1, 34-8, 2006.
23. Yilmaz, F., S. Dasdag, M. Z. Akdag, and N. Kilinc, "Whole-body exposure of radiation emitted from 900 MHz mobile phones does not seem to affect the levels of anti-apoptotic bcl-2 protein," *Electromagn. Biol. Med.*, Vol. 27, No. 1, 65–72, 2008.
24. Kim, T. H., T. Q. Huang, J. J. Jang, M. H. Kim, H. J. Kim, J. S. Lee, J. K. Pack, J. S. Seo, and W. Y. Pack, "Local exposure of 849 MHz and 1763 MHz radio frequency radiation to mouse heads does not induce cell death or cell proliferation in brain," *Exp. Mol.*

Med., Vol. 40, No. 3, 294–303, 2008.

25. Moquet, J., E. Ainsbury, S. Bouffler, and D. Lloyd, "Exposure to low level GSM 935 MHZ radio frequency fields does not induce apoptosis in proliferating or differentiated murine neuroblastoma cells," *Radiat. Prot. Dosimetry*, Vol. 131, No. 3, 287-96, 2008.
26. Saygin, M., S. Caliskan, N. Karahan, A. Koyu, N. Gumral, and N. Uguz, "Testicular apoptosis and histopathological changes induced by a 2.45 GHz electromagnetic field," *A. Toxicol. Ind. Health*, Vol. 27, No. 5, 455-63, 2011.
27. Mailankot, M., A. P. Kunnath, H. Jayalekshmi, B. Koduru, and R. Valsalan, "Radio frequency electromagnetic radiation (RF-EMR) from GSM (0.9/1.8 GHz) mobile phones induces oxidative stress and reduces sperm motility in rats," *Clinics*, Vol. 64, No. 6, 561-5, 2009.
28. Lee, H. J., J. K. Pack, T. H. Kim, N. Kim, S. Y. Choi, J. S. Lee, S. H. Kim, and Y. S. Lee, "The lack of histological changes of CDMA cellular phone-based radio frequency on rat testis," *Bioelectromagnetics*, Vol. 31, No. 7, 528-34, 2010.
29. Falzone, N, C. Huyser, D. R. Franken, and D. Leszczynski, "Mobile phone radiation does not induce pro-apoptosis effects in human spermatozoa," *Radiat. Res.*, Vol. 174, No. 2, 169-76, 2010.
30. Dasdag, S., M. Z. Akdag, E. Ulukaya, A. K. Uzunlar, and D. Yegin, "Mobile phone exposure does not induce apoptosis on spermatogenesis in rats," *Arch. Med. Res.*, Vol. 9, No. 1, 40-4, 2007.
31. Aydin, B. and A. Akar, "Effects of a 900-MHz electromagnetic field on oxidative stress parameters in rat lymphoid organs, polymorphonuclear leukocytes and plasma," *Arch. Med. Res.*, Vol. 42, No. 4, 261-7, 2011.
32. Lushnikov, K. V., A. B. Gapeev, V. B. Sadovniko, and N. K. Cheremis, "Effect of extremely high frequency electromagnetic radiation of low intensity on parameters of humoral immunity in healthy mice," *Biofizika.*, Vol. 46, No. 4, 753-60, 2001.
33. Quaglino, D., M. Capri, and I. P. Ronchetti, "Modulation of cell death in the rat thymus. Light and electron microscopic investigations," *Ann. N. Y. Acad. Sci.*, Vol. 926, 79–82, 2000.
34. Quaglino, D., M. Capri, L. Zecca, C. Franceschi, and I. P. Ronchetti, "The effect on rat thymocytes of the simultaneous in vivo exposure to 50-Hz electric and magnetic field and to continuous light," *Scientific World Journal.*, Vol. 4, Suppl. 2, 91-9, 2004.

35. Trelles, M. A., C. van der Lugt, S. Mordon, A. Ribé, and M. Al-Zarouni, "Histological findings in adipocytes when cellulite is treated with a variable-emission radio frequency system," *Lasers Med. Sci.*, Vol. 25, No. 2, 191-5, 2009.
36. De Felipe, I. and P. Redondo, "Animal model to explain fat atrophy using non ablative radiofrequency," *Dermatol. Surg.*, Vol. 33, No. 2, 141-5, 2007.
37. Vukova, T., A. Atanassov, and V. Ivanov, "Intensity-dependent effects of microwave electromagnetic fields on acetylcholinesterase activity and protein conformation in frog skeletal muscles," *Med. Sci. Monit.*, Vol. 11, No. 2, BR50-6, 2005.
38. Radicheva, N., K. Mileva, T. Vukova, B. Georgieva, and I. Kristev, "Effect of microwave electromagnetic field on skeletal muscle fibre activity," *Arch. Physiol. Biochem.*, Vol. 110, No. 3, 203-14, 2002.
39. Jin, P. Y., Y. W. Jo, S. I. Bang, H. J. Kim, S. Y. Lim, G. H. Mun, W. S. Hyon, and K. S. Oh, "Radiofrequency volumetric reduction for masseteric hypertrophy," *Aesthetic. Plast. Surg.*, Vol. 31, No. 1, 42–52, 2007.
40. Meltz, M. L., "Radiofrequency exposure and mammalian cell toxicity, genotoxicity, and transformation," *Bioelectromagnetics*, Supplement 6, 196–213, 2003.
41. Paniagua, J. M., R. Montaña, A. Jiménez, A. Antolín, and M. Sánchez, "Electrical stimulation vs thermal effects in a complex electromagnetic environment," *Science of the Total Environment*, Vol. 407, 4717–4722, 2009.
42. Markkanen, A., P. Penttinen, J. Naarala, J. Pelkonen, A.-P. Sihvonen, and J. Juutilaine, "Apoptosis induced by ultraviolet radiation is enhanced by amplitude modulated radiofrequency radiation in mutant yeast cells," *Bioelectromagnetics*, Vol. 25, 127–133, 2004.
43. Cao, Y., W. Zhang, M. X. Lu, Q. Xu, Q. Q. Meng, J. H. Nie, and J. Tong, "900-MHz microwave radiation enhances gamma-ray adverse effects on SHG44 cell," *J. Toxicol. Environ. Health A*, Vol. 72, Nos. 11–12, 727-32, 2009.